

# Frequency Hopping Wireless Power Transfer within the SAE J2954 operating frequency bandwidth - a concept design

*Graham Blankson*

Department of Electronic and  
Electrical Engineering  
Brunel University London  
Uxbridge, United Kingdom  
Graham.Blankson@brunel.ac.uk

*Mohamed Darwish*

Department of Electronic and  
Electrical Engineering  
Brunel University London  
Uxbridge, United Kingdom  
Mohamed.Darwish@brunel.ac.uk

*Chun Sing Lai*

Department of Electronic and  
Electrical Engineering  
Brunel University London  
Uxbridge, United Kingdom  
ChunSing.Lai@brunel.ac.uk

**Abstract** - The proliferation of electric vehicles (EVs) necessitates advancements in wireless power transfer (WPT) technologies to enhance security and efficiency. This paper introduces an enhanced Frequency Hopping Wireless Power Transfer (FHWPT) system designed within the Society of Automotive Engineers (SAE) J2954 recommended frequency bandwidth of 79kHz to 90kHz. The proposed FHWPT system utilizes frequency hopping to secure WPT operations against potential radio frequency interferences and cyber threats. The authors explore various mono resonant compensation circuit topologies and select the Series-Series topology for its simplicity and efficiency. An Impedance Matching Circuit (IMC) is integrated into both the transmitter and receiver circuits, enhancing the system's robustness by detecting misalignments and preventing power theft. Furthermore, the system dynamically selects operating frequencies using a microcontroller to manage interferences effectively, ensuring a resilient charging process. The paper confirms the potential of frequency hopping to improve the security and operational integrity of WPT systems for EVs.

**Keywords** – *Wireless power Transfer, Frequency Hopping, Impedance matching circuit, Radio Frequency interference.*

## I. INTRODUCTION

Frequency hopping is one of the techniques used for spectrum spreading in communications it is majorly used for avoiding interference while transmission by using narrow band channels within a given bandwidth in a sequential manner [1]. The SAE recommended an operating frequency bandwidth between 79kHz to 90kHz for wireless power transfer [2]. In the first

paper titled “Wireless Power Transfer System for Electric Vehicle Charging with Frequency Hopping – A Concept and Circuit Design.” [3] the FHWPT developed was limited to two frequencies (85kHz and 250kHz). This design required enhancement for three main reasons. Firstly, the SAE’s recommendation for WPT does not extend to 250kHz operating frequency for EV charging. Although the International Special Committee on Radio Interference - Publication 25, CISPR 25 stipulates the limits of electromagnetic interference (EMI) by electronic equipment for vehicles with operating frequencies between 0.15MHz - 5.925MHz. The theoretical calculations of the 100W WPT operating at 250kHz EMI is not representative of a 20kW, 50kW or 100kW EMI. Thus, implementing the design would have posed a risk of electromagnetic exposure to the user. Secondly, it was discovered that an oscilloscope can read the available binary frequencies of the FHWPT thus, limiting the redundancy and resilience of the transmission. As such the resilience and security of the dual operating frequency WPT system is limited. Thirdly, the calculated switching losses in the 100W WPT inverter driven by the NTB5860NL MOSFET operating at 250kHz was 3W i.e. 3% off the input power. On the other hand, when the 100W WPT is operating at 85kHz the switching losses are 1.61W, <2% of the input power. For these reasons, this paper presents a means to enhance the FHWPT to operate at multiple frequencies within 79kHz to 90kHz where the maximum operating frequency of 90kHz will dissipate a power loss of 1.67W.

## II. MONO RESONANT CIRCUIT TOPOLOGIES

Further studies were carried out to determine the mono resonant compensation circuit topology Series - Series (S-S) Series - Parallel (S-P), Parallel - Series (P-S) and Parallel - Parallel (P-

P) that will optimize the efficiency of the FHWPT. Fig 1 to 4 presents the mono resonant compensation circuits for the WPT. Table 1 details the total input impedances  $Z_{in}$  of the WPT where the secondary or receiver circuit impedances are referred in the primary or transmitter circuit for all topologies. The  $Z_{in}$  shall be programmed to the microcontroller to detect impedance

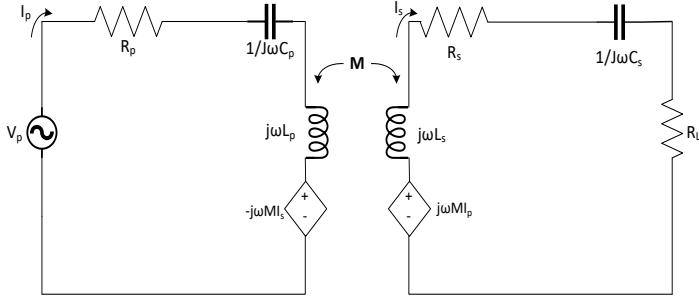


Fig. 1. Series – Series topology

mismatching during a charging session. The Series-Series topology was selected due to its simplicity, high Q factor, real power at resonance and simplistic computation of the impedance for the microcontroller [4].

In the S-S compensation topology, the  $Z_{in}$  is shown in (1) below.

$$Z_{in} = \frac{V_p}{I_p} = R_p + j \left( \omega L_p - \frac{1}{\omega C_p} \right) + \frac{\omega^2 M^2}{R_s + R_L + j \left( \omega L_s - \frac{1}{\omega C_s} \right)} \quad (1)$$

at resonance since the primary voltage  $V_p$  and current  $I_p$  are in phase there is no reactive energy, and the impedance is then simplified to

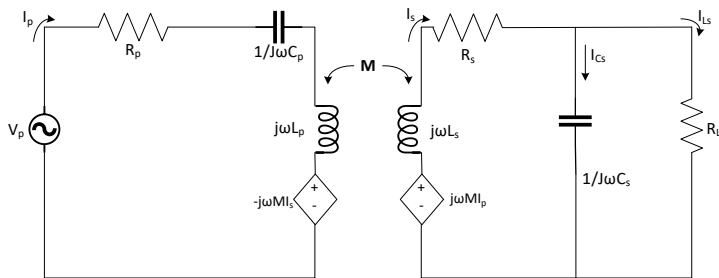


Fig. 2. Series – Parallel topology

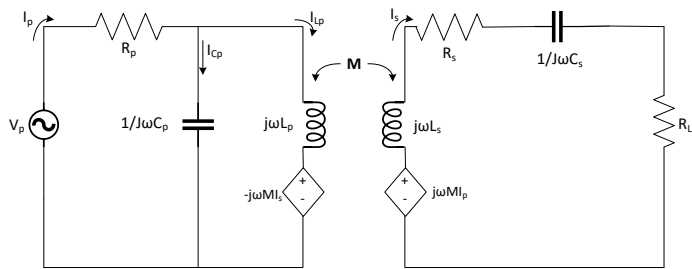


Fig. 3. Parallel – Series topology

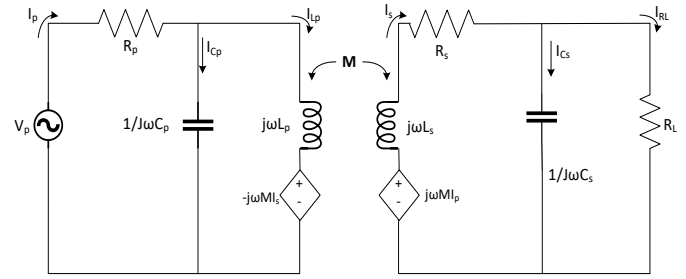


Fig. 4. Parallel - Parallel topology

$$Z_{in} = \frac{V_p}{I_p} = R_p + \frac{\omega^2 M^2}{R_s + R_L} \quad (2)$$

indicating that the  $Z_{in}$  is real and not reactive thus simpler to compute.

Topology	Input impedance
S-S	$Z_{in} = \frac{V_p}{I_p} = R_p + j \left( \omega L_p - \frac{1}{\omega C_p} \right) + \frac{\omega^2 M^2}{R_s + R_L + j \left( \omega L_s - \frac{1}{\omega C_s} \right)}$
S-P	$Z_{in} = \frac{V_p}{I_p} = \left( j \omega L_p - \frac{1}{j \omega C_p} \right) + R_p - \frac{\omega^2 M^2 (j \omega C_s R_L + 1)}{(R_s + j \omega L_s) (j \omega C_s R_L + 1) + R_L}$
P-S	$Z_{in} = \frac{V_{in}}{I_p} = \frac{\left[ (R_p + j \omega L_p) + \frac{\omega^2 M^2}{(R_s + j \omega L_s) + (j \omega L_s - \frac{1}{j \omega C_s})} \right]}{(1 + j \omega C_p) \left[ (R_p + j \omega L_p) + \frac{\omega^2 M^2}{(R_s + j \omega L_s) + (j \omega L_s - \frac{1}{j \omega C_s})} \right]}$
P-P	$Z_{in} = \frac{V_{in}}{I_p} = \frac{R_p + j \omega L_p + \frac{(j \omega C_s R_L + 1) j \omega M}{(R_s + j \omega L_s) (j \omega C_s R_L + 1) + R_L}}{j \omega C_s R_L + 1 \left( R_p + j \omega L_p + \frac{(j \omega C_s R_L + 1) j \omega M}{(R_s + j \omega L_s) (j \omega C_s R_L + 1) + R_L} \right)}$

Table I. Impedances of WPT mono resonant topologies

[5] developed input impedances for S-P, P-S and P-P topologies in their work indicating the presence of reactive energy due the reactive current in the parallel circuit which is out of phase with the input current.

**Table II. DESCRIPTION OF MONO RESONANT CIRCUITRY COMPONENTS**

Component designation	Function
$V_p$	Primary voltage
$I_p/I_s$	Primary/ Secondary current
$I_{cp}/ I_{cs}$	Primary/ Secondary capacitor current
$I_{Lp}$	Primary inductor current
$I_{RL}$	Load resistor current
$R_p/R_s$	Primary/ Secondary parasitic resistance
$R_L$	Load resistance
$Jw$	Angular frequency
$C_p/C_s$	Primary/ Secondary capacitor
$L_p/L_s$	Primary/ Secondary inductor
$M$	Mutual inductance

### III. IMPEDANCE MATCHING CIRCUIT

Impedance matching is a critical method of optimizing the throughput power between the source and the load [6] - [8] express impedance matching as a means to provide a conjugate match between the source impedance and load impedance implying that the impedance matching circuit (IMC) shall be in the WPT receiver circuit, however in the FHWPT the IMC shall be in both transmitter and receiver circuits to provide robustness and resilience.

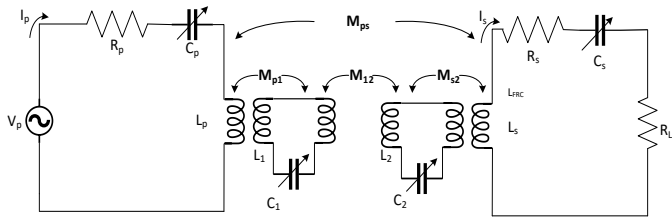


**Fig. 5.** Self Resonating Coil inductively coupled to transmitter and receiver coils.

Principally, the IMC is implemented as the detector of misalignments, power theft, presence of vehicle receiver, and internal impedance of the battery.

Secondly,  $L_1$  or  $L_2$  of the IMC in Fig 5 & 6 is the self-inductance of the self resonating coil (SRC) which by design is equivalent to the primary (transmitter)  $L_p$ , and secondary (receiver)  $L_s$ , side's coil self-inductance. These additional coils shall also optimize the power transfer efficiency (PTE) due to the increased flux linkage  $\Lambda$  with the transmitter/receiver coils as they act as a relay. [9].

$$\Lambda = N * \Phi. \quad (3)$$

Where  $N$  is number of turns, and  $\Phi$  is the flux. [10] highlighted that the energy transfer in an inductive coupled circuit is majorly influenced by the mutual inductance,  $M$ . From the formula

$$M = k\sqrt{L_p L_s}$$

(4)

where  $k$  is the coupling coefficient. It can be concluded that the increased number of turns increases  $k$ , thus increasing the PTE with the same input power. In the initial model a 40 turn spiral coil having a self inductance of 143.7uH was used thus, in this case the SRC will be 143.7uF almost doubling  $\Lambda$  and significantly increasing  $k$  and  $M$  for the same input power.

Thirdly, the SRC consisting of,  $L_1$  and  $L_2$  and their respective capacitive banks  $C_1$  and  $C_2$  see Fig. 5, 6 & 7, shall be regulated to operate at the resonant frequency of the transmitter/receiver coils  $L_p$  and  $L_s$ .

### IV. CONTROL

Data from the mutual inductances  $M_{WPT}$ , between the primary and secondary coils  $M_{ps}$ , the primary coil and primary SRC  $M_{p1}$ , the primary and secondary SRC  $M_{12}$ , and the secondary coil and secondary SRC  $M_{s2}$ , of the WPT shall be monitored during the charging session. The magnitude of  $M_{WPT}$  at steady state, few seconds into normal operation, shall be set as a reference  $M_{ref}$ . The microcontroller will consistently compare the monitored  $M_{WPT}$  with  $M_{ref}$  to determine the loss of line of sight or misalignments and presence of a legal or illegal inductive loads.

The Q factor  $\frac{R}{\omega L}$ , of the transmitter and receiver coils shall be processed respectively to determine the operational status of the WPT. Q factor data shall be used to validate the change of frequency whilst the  $M$  shall be used to detect misalignments and near field receivers (power theft).

The SRC will be used as an antenna to detect radio frequency (RF) interference signals. The microcontroller shall be programmed to determine changes in the phase, frequency, or amplitude of the original transmission signal of the transmitter and receiver circuits. The microcontroller shall measure the Signal to Noise Ratio (SNR) to underpin the resilience of the WPT.

$$SNR_{dB} = 10 \log_{10} \left( \frac{\text{Signal power}}{\text{Noise Power}} \right)$$

The SNR will detect any ipsilateral interferences [11].

To further reinforce the WPT to detect and ride through RF interferences the RF monitoring shall also be carried out using

the received signal strength indicator equation (RSSI) equation [12]

$$RSSI = P_t - P_l(r0)$$

Where  $P_t$  is signal transmit power,  $P_l(r0)$  is signal received strength. The SNR and RSSR parameters shall be calculated at the start and continuously over a charging session using. To make the system sensitive enough to avoid nuisance tripping a 1% tolerance of the SNR and RSSI limit shall be programmed in the microcontroller FH instruction set. A 1 second delay shall also be introduced in the microcontroller to damp the FH response. If the SNR and RSSI limits are breached during a charging session the FH shall be initiated.

A Bluetooth or ZigBee shall be used to transmit the Q or operating frequency of the transmitter to the receiver circuit. It is expected that the transmitter circuit's operating frequency shall be communicated to the receiver's circuit via ZigBee.

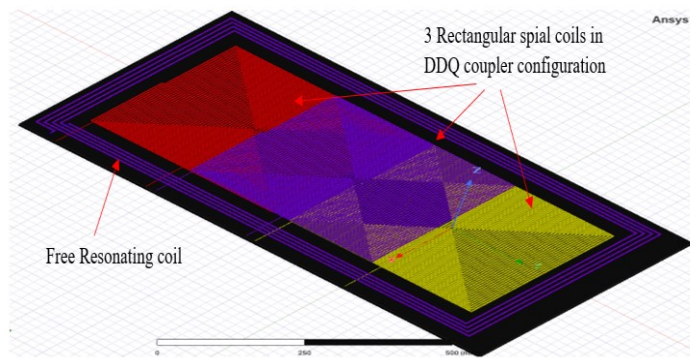


Fig. 6. double D Q (DDQ) coil and SRC coil configuration.

## V. FREQUENCY HOPPING

It is expected that when an interference is detected the microcontroller will instruct the frequency selector circuit (FSC) [3] to hop to an alternative operating frequency [3] within the SAE's frequency bandwidth. The FSC has twelve 1kHz bandwidth channels thus, enabling the operating frequency to hop between 79kHz and 90kHz. The FSC achieves this by regulating the variable capacitors  $C_p$  and  $C_1$  in the EV charger's

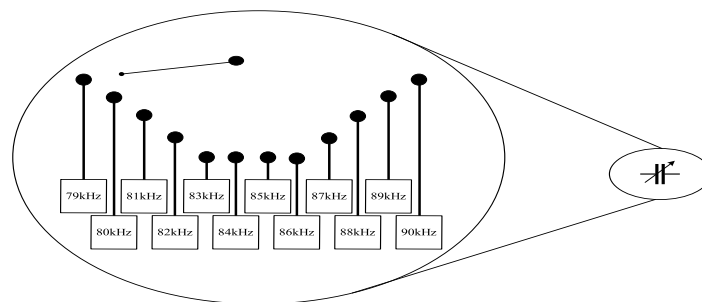


Fig. 7. Variable capacitors  $C_p$ ,  $C_1$ ,  $C_2$ ,  $C_s$  array facilitating 12 channels for frequency hopping between 79kHz and 90kHz

transmitter and  $C_2$ , and  $C_s$  in the EV's receiver. Data from the transmitter and receiver unit's microcontroller is exchanged via Zigbee Wi-Fi [3] to enable the autonomous units work in tandem. The dynamic response of the WPT shall be quick enough to maintain the standard period of a charging session.

The FHWPT is not limited to detecting various types of interference but also able to recognize the profile of the source. This is achieved by coding algorithms that compute the total harmonic distortion (THD) and RSSI caused by the interference.

If a broad spectrum frequency jammer interferes a charging session the IMC can determine its characteristics by hopping through series of frequencies and measuring the distortions on those channels. In cases where there is a broad spectrum attack the WPT shall notify the user and with the help of CCTV surveillance in the vicinity the perpetrator can be accosted.

The flow chart in Fig. 8. presents the processes which the microcontroller undertakes before and during the charging session. It is expected that the FHWPT's default operating frequency is set to 85kHz. To save energy the FHWPT does not switch on until an EV is present. If the EV's operating frequency is detected via Zigbee Wi-fi the FHWPT will set to the EV's operating frequency if its not 85kHz else it will notify the user of the issue and return to standby by mode. Once charging commences  $M_{WPT}$  would be monitored to check for misalignments or loss of line of sight. If any anomaly is detected FHWPT will notify user and stop operation. If RF interference is detected the FHWPT will attempt to identify the RF profile then hop to the next channel if the issue persists this FHWPT will hop through all channels. If the RF interference affect all channels then the user and security are notified a possible cause would be a broad spectrum jammer. If the interference just affects few channels the FHWPT will switch to the secure channel. Another check done by the FHWPT is the output power level if this is within the limits charging continues else the user and security are notified and the charging stops as there is a possible power theft.

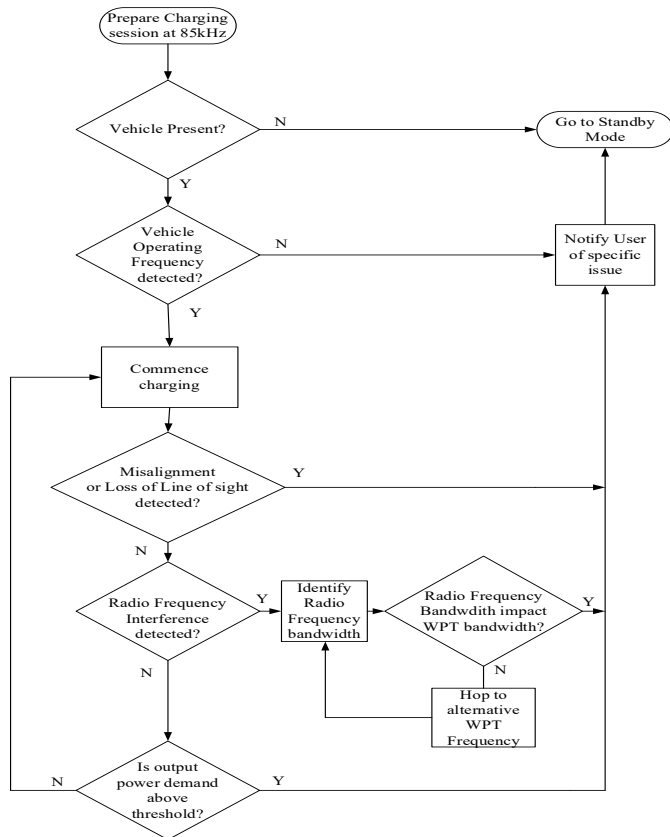


Fig. 8. Flow chart of Frequency hopping

## VI. Conclusions

This paper presents the development of an enhanced FHWPT system that operates within the SAE recommended frequency bandwidth of 79kHz to 90kHz. This system is designed to secure wireless power transfer (WPT) operations from a broad range of interferences while maintaining safety integrity. The paper explored various mono resonant compensation circuit topologies and selected the Series-Series (S-S) topology due to its simplicity, high Q factor, and the ability to produce real power at resonance, which simplifies impedance calculations. The Impedance Matching Circuit (IMC) has been integrated into both the transmitter and receiver circuits of the FHWPT system to enhance robustness and resilience. It is used for detecting misalignments, power theft, and ensuring efficient power transfer.

The work presented in this paper uses a microcontroller to dynamically select and hop between multiple frequencies within the designated bandwidth in response to detected interferences. This ensures the resilience of the WPT system against radio frequency interferences and potential cyber threats. The paper suggests future work to develop a modular capacitor bank, self-resonating coil (SRC), and frequency hopping (FH) controller that can be retrofitted into existing wireless EV chargers to enhance their security and efficiency.

The paper indicates that the FHWPT system's effectiveness in handling interferences and maintaining operational integrity

during electric vehicle (EV) charging sessions is validated through the implementation of the frequency hopping mechanism.

In general, the paper concludes that the proposed enhancements to the FHWPT system provide a robust solution to secure wireless power transfers for electric vehicles against various types of interferences while maintaining high efficiency and safety standards.

## VII. REFERENCE

- [1] Handbook of RF and Wireless Technologies F. Dowlia <https://doi-org.ezproxy.brunel.ac.uk/10.1016/B978-0-7506-7695-3.X5000-9> ISBN 978-0-7506-7695-3
- [2] A. Vulfovich and A. Kuperman, "Relation Between Operation Frequency Range and Coupling Coefficient Variations in WPT Under Subresonant Frequency Control," *2021 IEEE PELS Workshop on Emerging Technologies: Wireless Power Transfer (WoW)*, San Diego, CA, USA, 2021, pp. 1-5, doi: 10.1109/WoW51332.2021.9462891.
- [3] G. Blankson, M. Darwish and C. S. Lai, "Wireless Power Transfer System for Electric Vehicle Charging with Frequency Hopping – A Concept and Circuit Design," *2023 58th International Universities Power Engineering Conference (UPEC)*, Dublin, Ireland, 2023, pp. 1-6, doi: 10.1109/UPEC57427.2023.10294567
- [4] M. Singh, S. Samanta and S. P. Das, "A Generalized Method of Determining Coil and Compensation Circuit Parameters of Basic WPT Topologies," *2021 National Power Electronics Conference (NPEC)*, Bhubaneswar, India, 2021, pp. 1-6, doi: 10.1109/NPEC52100.2021.9672507.
- [5] A. Triviño-Cabrera, J.M. González-González, J.A. Aguado "Fundamentals of wireless power transfer," in: *Wireless power transfer for Electric Vehicles: foundations and design approach*. Switzerland: Springer, 2020, 1-18.
- [6] D. Misra, *Radio-Frequency and Microwave Communication Circuits: Analysis and Design*, New Jersey: John Wiley & Sons, Inc, 2004
- [7] A. P. Putra and A. Munir, "Impedance matching circuit for 30–88MHz monopole antenna with automatic matching," *2015 1st International Conference on Wireless and Telematics (ICWT)*, anado, Indonesia, 2015, pp. 1-4, doi: 10.1109/ICWT.2015.7449247.
- [8] A. Mohan and S. Mondal, "An Impedance Matching Strategy for Micro-Scale RF Energy Harvesting Systems," in *IEEE Transactions on Circuits and Systems II: Express Briefs*, vol. 68, no. 4, pp. 1458-1462, April 2021, doi: 10.1109/TCSII.2020.3036850.
- [9] D. -W. Seo, "Comparative Analysis of Two- and Three-Coil WPT Systems Based on Transmission Efficiency," in *IEEE Access*, vol. 7, pp. 151962-151970, 2019, doi: 10.1109/ACCESS.2019.2947093.
- [10] Porto, Rodrigo Wolff & Brusamarello, Valner & Müller, Ivan & Sousa, F.R.. (2015). Design and characterization of a power transfer inductive link for wireless sensor network nodes. *Conference Record - IEEE Instrumentation and Measurement Technology Conference*. 2015. 1261-1266. doi: 10.1109/I2MTC.2015.7151454.
- [11] P. Wang, Y. Sun, Y. Feng, T. Feng, Y. Fan and X. Li, "An Improvement of SNR for Simultaneous Wireless Power and Data Transfer System With Full-Duplex Communication Mode," in *IEEE Transactions on Power Electronics*, vol. 37, no. 2, pp. 2413-2424, Feb. 2022, doi: 10.1109/TPEL.2021.3106903
- [12] A Received Signal Strength based Self-adaptive Algorithm Targeting Indoor Positioning Xiaoyue Hou, Tughrul Arslan, Arief Juri University of Edinburgh. <https://www.ewireless.eng.ed.ac.uk/sites/ewireless.eng.ed.ac.uk/files/attachments/A%20Received%20Signal%20Strength%20based%20Self-adaptive%20Algorithm%20Targeting%20Indoor%20Positioning.pdf>